IEEE Access
Multidisciplinary | Rapid Review | Open Access Journal

Received 20 March 2024, accepted 14 May 2024, date of publication 22 May 2024, date of current version 3 June 2024.

Digital Object Identifier 10.1109/ACCESS.2024.3403988

RESEARCH ARTICLE

Performance Evaluation of Thailand's 8 MW Wind Farm Feeder Trip, Energy Generation, and Loss Using 5 MWh BESS–A Statistical and Economic Approach

RATTAPORN NGOENMEESRI[1], SIRINUCH CHINDARUKSA[1,2], RABIAN WANGKEEREE[3], AND CHATCHAI SIRISAMPHANWONG[1,2,4]

[1]Department of Physics, Faculty of Science, Naresuan University, Phitsanulok 65000, Thailand
[2]Smart Energy System Integration Research Unit, Department of Physics, Faculty of Science, Naresuan University, Phitsanulok 65000, Thailand
[3]Research Center for Academic Excellence in Mathematics, Department of Mathematics, Faculty of Science, Naresuan University, Phitsanulok 65000, Thailand
[4]Research Center for Academic Excellence in Applied Physics, Faculty of Science, Naresuan University, Phitsanulok 65000, Thailand

Corresponding author: Chatchai Sirisamphanwong (chatchaisi@nu.ac.th)

ABSTRACT In this study, an operational 8 MW wind farm was analyzed through a statistical approach to determine the wind speed and feeder trip correlation with energy loss and energy production. In December, a higher wind potential was recorded; however, a higher feeder trip was recorded during the low wind potential period of October, with a maximum duration of 1800 min. The box plot and histogram show that a higher feeder trip occurred at a wind speed of 4-6 m/s, indicating that grid voltage and load consumption were the major causes of the feeder trip. The Pearson Correlation method expressed a similar trend for feeder trips associated with energy losses that had a strong positive correlation compared to feeder trip time. To improve the stability of the wind farm's power generation, a 1-5 MWh battery energy storage system was studied to determine its impact on the grid voltage at the wind farm and the load terminals. It was found that 411071.84 kWh is enhanced for a 5 MWh battery energy storage system compared to the conventional wind farm. This enhancement in power production shows a positive correlation of grid voltage at the factory, village 1, wind farm, village 2, and village 3 with a range of 0.703, 0.873, 0.665, 0.894, and 0.896, respectively. Further, the economic analysis of the 5 MWh battery incorporation increased the annual revenue to 2825585 baht with a payback period of 7.79 years and a return on investment of 0.10 years.

INDEX TERMS Feeder trip, energy generation, energy loss, statistical analysis, economic benefit, payback period.

NOMENCLATURE

ADALINE	ADAptive Linear Neuron.
ASFR	Aggregated System Frequency Response.
BCR	Benefit-Cost Ratio.
BESSs	Battery Energy Storage Systems.
DTA04	Voltage at Factory.
EL	Energy Loss.
EP	Energy production.
E-o-L	End-of-Life.
FL	Fuzzy Logic.
FT-No	Feeder Trip Number/count.
FT-T	Feeder Trip Time.
GA	Genetic Algorithm.
IQR	Interquartile Range.
IRR	Internal Rate of Return.
Li-ion	Lithium-ion.
MPC	Model Predictive Control.
NASA	National Aeronautics and Space Administration.
NPC	Net Present Cost.

The associate editor coordinating the review of this manuscript and approving it for publication was Ton Duc Do.

NPV	Net Present Value.
PCC	Point of Common Coupling.
PCC_01	PCC voltage at Village 1.
PCC_02	PCC voltage at Village 2.
PCC_03	PCC voltage at Village 3.
PF	Power Factor.
PP	Payback Period.
Q	Quartile.
RESs	Renewable Energy Sources.
SD	Standard Deviation.
Va-Red/VRB	Vanadium-Redox/Vanadium-Redox Battery.
VSPP	Very Small Power Producer.
wb	With BESS.
wob	Without BESS.
WS	Wind Speed.
X_i, Y_i	individual wind power production/loss (X) and feeder trip (Y).
$\bar{X}$, $\bar{Y}$	means of wind power production/loss and feeder trip.

I. INTRODUCTION

Environmental pollution has become a significant concern in modern society, and 220 Mt of CO_2 is produced during electrical and heat energy conversion. Renewable Energy Sources (RESs) are efficient for reducing fossil fuel consumption and directly controlling pollution [1], [2]. Several RESs in practice among wind energy generation have gained popularity as they have high energy density and require less area for implementation [3], [4]. Although wind energy is an abundant resource, it fails to meet the load requirements owing to discontinuous power generation and over/low voltage productions. Voltage fluctuations occur on the variability of wind speed and are directly dependent on natural occurrence [5]. Several factors affect wind speed, such as atmospheric pressure, geographical conditions, seasonal changes in sunlight, hurricanes, and wind shear. These occurrences are not controllable, but it is predictable to solve voltage fluctuations during the grid feed [6]. Apart from natural occurrences, voltage fluctuations occur due to poor load management. During peak load demand periods, if unexpected load consumption occurs, the higher current drawn from the distribution and transmission line decreases the grid voltage. A higher grid voltage occurs when the estimated load demand is not met during the higher wind speed period [7], [8].

In most cases, the voltage regulator maintains the grid voltage within the allowable range. However, voltage regulators cannot handle sudden fluctuations in wind speed and load consumption, resulting in a lagging Power Factor (PF) [9], [10]. Battery Energy Storage Systems (BESSs) have been widely employed to overcome voltage fluctuations and reduce active power curtailment. The BESS regulates the grid frequency and smoothens the output power by storing excess energy from wind turbines [11], [12]. Subsequently, the BESS discharged when the grid voltage was lower than the predicted/actual range. The BESS favors the maintenance of grid balancing, grid resilience, and peak power shaving [13]. However, integrating a BESS with wind turbines cannot resolve the grid frequency mismatch without a proper response system. To optimize the BESS capacity, a history of the load and energy profiles is required [14].

Furthermore, wind turbine operating characteristics such as wind speed, seasonal wind variation, and other maintenance charts are required. Based on these analyses, the BESS capacity was determined using advanced energy-management systems. Prioritizing BESS's charging and discharging characteristics could reduce the active power curtailment and favor an attractive Payback Period (PP) of the system [15]. Further, this study reviewed BESS-associated wind turbines to understand their economic viability.

Optimizing BESS's capacity is a significant challenge in wind energy systems, as it requires real-time operational parameters of a wind turbine, grid network, and its distortion during distribution. Second, they determine the impact of BESS operations on grid stability and network performance [16]. The dual-power ramp strategy controls the required amount of power injected into the grid and reduces the BESS capacity [17]. ADAptive Linear Neuron (ADALINE) effectively tracks the wind farm's power production and responds quickly to power fluctuation. A dual constraint implementation to ADALINE protects against the unexpected increase/decrease in the combined power output of BESS and wind farms. This technique smoothens the 99 MW wind farm power production using a 12.13 MWh BESS [17]. Following this, multi-layer optimization techniques were developed by Jannati and Foroutan [18], considering the discontinuous/intermittent nature of wind power production. The flexible ADALINE method uses linear prediction and particle swarm optimization algorithms to monitor power production. The power feed was controlled without deteriorating the grid frequency and excess energy stored in the BESS. To compensate for the voltage fluctuation, the heuristic algorithm tracks the charging and discharging characteristics of the BESS, which helps extend its operation and lifetime.

Liu et al. [19] developed complex modeling and control strategies to understand BESS operations' nonlinear and stochastic nature, as the power and energy density are inversely proportional. Multi-objective optimization is crucial in monitoring the BESS's power and energy density, and the Model Predictive Control (MPC) mechanism regulates BESS charging and discharging to the grid. It was found that 30% of the power feed to the grid is increased, and controlled thermal management for BESS increases the operational lifetime compared to the existing BESS. Song et al. [20] developed a multi-objective optimization algorithm and categorized the process into initialization, evaluation, selection, and reproduction. This technique uses the BESS degradation rate and thermal effects to assess the system performance. Population size, crossover rate, and mutation rate play a crucial role in the operation of the

Genetic Algorithm (GA) and Fuzzy Logic (FL) to reduce uncertainty. The developed algorithm provides energy savings, increases utilization of renewable energy, and reduces peak load demand by 23.7%, 18.5%, and 15.3%, respectively.

Several studies have stated that the DIgSILENT PowerFactory is a reliable and efficient tool for optimizing BESS capacity and distributed power generation using a dynamic simulation [21], [22], [23]. It is mainly used to perform a simple analytical model and load-shedding approaches for a quick response in frequency regulation. Emon et al. [24] performed Aggregated System Frequency Response (ASFR) modeling to monitor the frequency deviation, frequency nadir, and rate of change of frequency to improve grid frequency stability using BESS. Subsequently, ASFR combined with the second-order approximation method evaluates the frequency nadir using actual frequency data and concludes that the required capacity of BESS is 0.5-2.5% of wind turbine rated capacity. Comparatively, this technique recommends the lowest BESS capacity among the methods by maintaining the system frequency response. As mentioned earlier, optimizing the capacity of BESS is a significant task, especially regarding the economic aspect, as an increase in the capacity of BESS increases the return on investment. Several studies state that BESS internal losses, such as performance degradation, thermal-oriented operational stress, and improper power management, affect system efficiency [25], [26], [27].

Youseef et al. [28] generated the actual power generation from PV and wind; input parameters are obtained from the National Aeronautics and Space Administration (NASA), and real-time resources are used for biomass. Lithium-ion (Li-ion) and lead-acid batteries are used to store excess energy from the above-mentioned renewable energy generators. Notably, lead-acid batteries show a lower initial investment than Li-ion; however, operating costs are high. Net Present Cost (NPC) is high for PV/wind/biomass integrated with lead-acid batteries. On the other hand, PV/wind, PV/biomass, and PV-alone with Li-ion show higher NPC. Subsequently, Niaz et al. [29] optimized the BESS for the Tehran, Iran location to minimize power curtailment and maintain the grid frequency. Historical data on wind farms, load profiles, and other environmental parameters were collected from the Iranian Renewable Energy Organization to train the developed model. To assess the economic impact on the system, power curtailments of 25%, 50%, 75%, and 100% were performed using a 50 MW/600 MWh BESS. It was found that operating the renewable energy system with 100% BESS mode failed to reduce the power curtailment. Renewable energy generation, including PV, wind, and biomass, is used to optimize the BESS under various operating conditions on an island.

Similarly, Niaz et al. developed a hybrid energy storage system for a standalone system in a rural area of Egypt, and the examined renewable energy generator faces 8% to 12% power curtailment. It was found that the BESS reduced power curtailment by 5 %, which increased revenue by 7%. The PV and wind turbines generate 9874.71 kWh for the Ras Ghareb location, and the BESS with water electrolyzer power generation reached 16,984.51 kWh. For the Mersa Matrouh and Aswan regions, annual energy generation was enhanced by 26.62% and 27.28 %, respectively. The Mersa Matrouh and Aswan regions attained higher economic benefits than Ras Ghareb owing to seasonal variation in renewable energy generation [30].

The economic viability of BESS integration varies depending on the location and the local grid power purchasing agreement. Lobato et al. [31] evaluated the economic viability of BESS for a 30 MW wind farm in the Spanish market. In this case, Li-ion and Vanadium-Redox (Va-Red) are used to evaluate the economic feasibility as BESS initial investment cost and efficiencies are not the same, but end-of-life (EoL), EoL efficiency, and number of cycles per day are the same. Although the integration of BESS favors the wind farm to deliver smooth power output, it did not result in a remarkable economic change. The reason for this non-drastic improvement is that the international coordination of automated frequency restoration and stable system operations is under construction.

From the above literature and Table 1, integrating BESS favors smoothing the power delivery, improving the grid stability, and reducing the power curtailment. The performance of the BESS with a wind farm varies depending on the local grid load profile and energy generation, which makes optimizing the capacity of the BESS a necessary measure to attain a higher efficiency of the system. Second, the economic viability of BESS integration is different for each location, and it is truly dependent on the local grid power purchasing agreement. To the author's knowledge, no study has been conducted on optimizing the BESS for Thailand's wind farm on economic aspects. Considering this research gap, in this study, BESS optimized following our previous study [32], and the power generation was statistically analyzed to determine the reliability of the developed system. Furthermore, economic feasibility was determined under real-time operating conditions.

II. MATERIALS AND METHODS

A. STATISTICAL ANALYSIS

Statistical methods are widely used to uncover the patterns and trends of systems. This study analyzed wind farm power generation and losses using annual wind speed and feeder trip data.

1) WIND SPEED

The discontinuous wind speed pattern was analyzed using a box plot and histogram view every month to determine the root cause of power deterioration. Box plots are presented in whiskers and Interquartile Range (IQR). In the wind speed data, 50% of high values are shown as IQR split into three segments: Q1, Q2/median (horizontal partition of the box), and Q3. The IQR bottom box represents 25% of the wind speed from 50% of IQR; the median and Q3

TABLE 1. Recent literature of renewable energy system with energy storage.

Location	Renewable energy generator capacity	BESS capacity	Energy benefit with BESS	BESS cost	Payback period	Reference
United Kingdom	-	1.25 GWh	£0.040/kWh	200 £/kWh	14 years	[33]
China	Wind 200 MW PV 50 MW	125 MWh	-	-	-	[34]
Germany	-	20 MWh	-	-	9.25 years	[35]
China	PV 1 MW	3.78 MWh	-	1800 yuan/ kWh	6.9 years	[36]
China	Wind 20.745 MW PV 17.338 MW	Li-ion 14 GWh VRB 15.6 GWh	Li-ion 0.086 yuan/MWh VRB 0.144 yuan/MWh	Li-iom ESS 2000 yuan/kWh VRB ESS 3000 yuan/kWh	-	[37]
South Africa	PV/Wind microgrid	30 kW	$0.847/kWh	$74,609	-	[38]
United Nations	PV 8.67 kW	7 kWh	0.34/kWh	$25,099	-	[39]
Italy	PV 40 kW	145 kWh	-	450 €/kWh	-	[40]
Cyprus	PV 2.89 MW Wind 1.15 MW	2.31 MWh	0.1838 €/kWh.	-	-	[41]
Thailand	PV 3.9 kW	32 kWh	0.245 $/kWh	$134 / kWh	-	[42]
-	PV 1.523 MW Wind 1.785 MW	360.2 kWh	-	$0.5187 M	-	[43]
Egypt	PV 126.14 kW Wind 100 kW	-	0.118 $/kWh	$ 65,015	-	[44]
Span	Wind 30 MW	2.5 MWh	-	11,000 €/MWh	-	[31]
China	Wind and PV	6860.91 kWh	-	-	-	[45]
China	Wind 99 MW	10 MW / 0.3 MWh	-	-	-	[46]
China	Wind 2 MW	1 MWh	0.0340$/kWh	123,000 $	3.5 years	[47]
China	Wind 153 MW	-	-	946,100 yuan	-	[48]
China	Wind 360 kW PV 260 kW	700 kWh	-	-	-	[49]
China	Offshore wind	Pumped storage 240 MW	-	243,000 CNY	-	[50]
Canada	Wind 200 kW	100 kWh	-	-	-	[51]
China	Wind	Lithium 6.80 MWh Flywheel 0.3204 MWh Supercapacitor 0.1026 MWh	-	$7.5647x10^5$ CNY	-	[52]
China	Wind 22 MW	Battery 10.44 MWh Supercapacitor 10 MWh	-	Battery 930 yuan/kW Supercapacitor 12400 yuan/kW	-	[53]
Libya	Wind 30 kW PV 30 kW	Hydrogen storage	0.137 $/kWh	Electrolyzer 900 $/kW Compressor 1800 $/kW	7 year	[54]
United States	Offshore Wind 350 MW	Compressed Air Energy Storage (OCAES) 200 MW	$0.22/kWh	$1457/kW	-	[55]
Thailand	8 MW	5 MWh	411071.84 kWh/year	Wind farm = 103,057,495/MW BESS = 15,000 baht/kWh	7.89 years	Present study

are 50% and 75%, respectively. Apart from the box, the lower and upper whiskers denote the minimum and maximum wind speeds of Q1-1.5×IQR and Q3-1.5×IQR, respectively. The Histogram view is a summarized representation of the dataset frequency for wind speed. It is widely used to analyze the frequency distribution of continuous datasets. The X-axis and Y-axis represent the wind speed and frequency distribution of the wind speed, respectively.

2) FEEDER TRIP

The primary issue in wind farms is the feeder trip, which disconnects wind turbine power generation from the distribution system. Unpredicted and lack of power distribution attributed to feeder trips. Feeder trip patterns were analyzed using a histogram to understand the nature of the selected wind farm operations against load consumption. Feeder trip frequency distributions were categorized into different scenarios

concerning the wind speed of the location, the wind turbine's operational time, and the feeder trip's total duration.

3) POWER PRODUCTION AND POWER LOSS

Pearson correlation is widely used to assess the strength and direction of two linear variables as expressed in Eq. (1). In this case, a correlation between the power production and feeder trip and how the feeder trip increased the power loss was studied. Furthermore, the different capacities of BESS with 8 MW wind farm annual power generation were studied to understand the benefit of BESS integration. The correlation coefficient is expressed in the range of -1 to $+1$, where -1 and $+1$ indicate a strong negative and positive correlation between the two variables, respectively, and 0 indicates no correlation.

$$Pearson\ correlation,\ r = \frac{\sum \left(X_i - \bar{X}\right)\left(Y_i - \bar{Y}\right)}{\sqrt{\sum \left(X_i - \bar{X}\right)^2 \sum \left(Y_i - \bar{Y}\right)^2}} \quad (1)$$

where, X_i, Y_i = individual wind power production/loss (X) and feeder trip (Y). $\bar{X}$, $\bar{Y}$ = means of wind power production/loss and feeder trip.

4) LOW AND HIGH LOAD PROFILE

Feeder trips occur during low- and high-voltage periods due to load demand fluctuations. To determine the relationship between the feeder trip and the voltage profile, a Pearson correlation was performed on the specific periods of low- and high-load profiles of the wind farm. A comparative correlation between the voltage profiles with and without BESS was conducted for both load profiles.

B. ECONOMIC ANALYSIS

Economic analysis is predominant in convincing policymakers, stakeholders, and individuals to install wind energy systems. It is well known that wind energy systems efficiently deliver renewable power generation with an attractive return on investment. Under certain circumstances, wind energy systems fail to meet economic benefits, especially when the system is not commissioned correctly as per the local grid regulations. In this case, an 8 MW wind turbine is commissioned following the Thailand grid regulations; however, unexpected load demand increases power curtailment. Second, active power curtailment raised concerns about wind turbine manufacturers' warranties owing to higher feeder trips. As per the wind turbine manufacturer, feeder trips must not exceed 52 times a year; unfortunately, they reach 146 times. In our previous study, different capacities of BESS were approached to reduce the feeder trip, and the same methodology was followed for this study.

Furthermore, the economic viability of the proposed BESS with wind turbine power generation was discussed. The major parameters used to evaluate the economic benefits of the proposed system were **Net Present Value (NPV), Internal Rate of Return (IRR), Benefit-Cost Ratio (BCR), and Payback Period (PP).** A description of the selected 8 MW wind farm is listed in Table 2.

TABLE 2. General information about the Subplu project.

Content	Description
Project shareholder	Wind Energy Development Co., Ltd.
Project location	Ban Huai Bong, Dan Khun Thot District, Nakhon Ratchasima Province, Thailand
Installed capacity	8 MWp
Wind turbine model	Gamesa G114-2.0MW
Power purchaser	Provincial Electricity Authority (PEA)
Power purchase duration	10 years + 10 years
Electricity selling structure	electricity tariffs + FT + Adder
Date of plant operation	March 17, 2016

III. RESULTS AND DISCUSSIONS

An 8 MW wind farm from Nakhon Ratchasima Province, Thailand, has been operational since March 17, 2016. The Provincial Electricity Authority of Thailand commissioned the wind power plant to minimize conventional power generation and mitigate grid power demand. Wind energy is discontinuous/intermittent in power generation and predictable. However, it is not easy to maintain a balanced grid power flow because it directly relies on the power consumption in the grid. Figure 1 shows the annual box plot of wind speed for the 8 MW wind farm in Nakhon Ratchasima Province, Thailand. The cross-lined box represents 50% of the wind speed every month, and the lower and higher 25% of wind speeds are shown as whiskers. An increase in the length of the horizontal box indicated a wide variation occurring at 50% of the wind speed. In January, a higher box length was recorded, starting from 3.54-8.39 m/s, which means that 50% of the wind speed lies between these ranges. An increase in the box length did not effectively favor attaining high power generation, although it was better than that in March, April, May, and September. A box plot such as the IQR must attain a smaller box length in a higher wind speed region for effective power generation.

This state indicates that the oscillation of wind speed is lower for 50% of the monthly wind speed, and it attained a higher wind speed, resulting in stable power generation. Comparatively, March, April, May, and September contain small box lengths, but they attain lower power generation in the lower wind speed region. During December, 50% of the wind speed was recorded to be 5.46-9.12 m/s, and the median/Q2 is 7.57 m/s, making this month have a high potential for energy generation. Following December, a similar wind speed pattern was recorded in July and June. December, July, and June were categorized as having the highest potential periods. November, January, August, and February are moderate potential periods, and March, April,

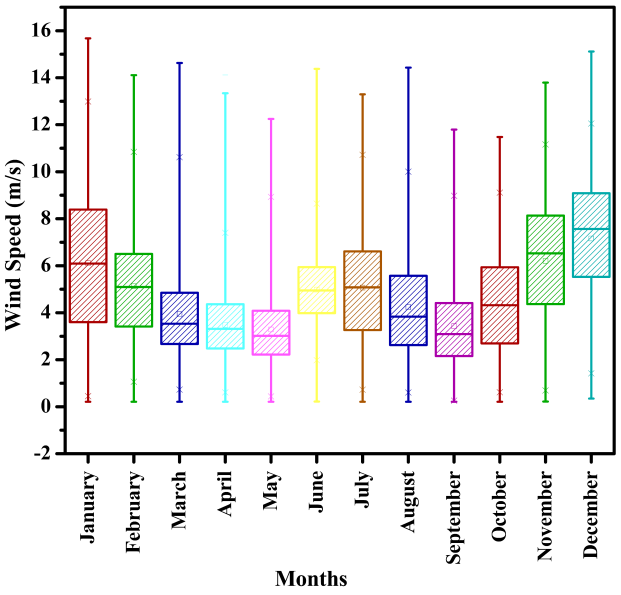

FIGURE 1. Box plot representation of annual wind speed for an 8 MW wind farm.

May, September, and October are low potential periods for wind-power generation.

In a standardized way, commercial wind farms monitored by Supervisory Control and Data Acquisition (SCADA) measure the wind speed by 10 minutes to obtain a manageable dataset [56], [57]. To further understand the nature of wind speed, monthly categorized annual wind speeds were analyzed using a histogram. The high wind potential period of December attained a higher wind speed of 7-9 m/s more than 650 times. Following that, the second highest period of July showed a wind speed of 6-7 m/s more than 680 times. Between 3-7 m/s, the wind speed was sustained more than 500 times. After 7 m/s, the wind speed failed to maintain a higher frequency count and was slowly reduced. Comparatively, a higher frequency count of more than 1100 times was recorded for June with a wind speed of 4-5 m/s. However, June failed to compete in terms of higher power production with December and July due to fluctuations in wind speed, as shown in Figure 2. January gained a stable wind speed compared to other months; however, the frequency of the wind was not as high as that of the months mentioned above. Notably, 4 m/s and 9 m/s wind speeds were recorded for more than 500 frequency counts. The primary benefit of the January wind speed is that more than 400 counts are recorded at 2-9 m/s separately, which is predominant in producing moderate power with a lower oscillation. Subsequently, November recorded similar wind patterns with 7-9 m/s for more than 590 counts. August marked a sudden sweep in wind speed after 5 m/s and attained less than 400 counts, while February had the least wind power conversion potential in a moderate wind speed period. As mentioned earlier, March, April, May, September, and October are low potential periods, as it can be seen that during March, a wind speed

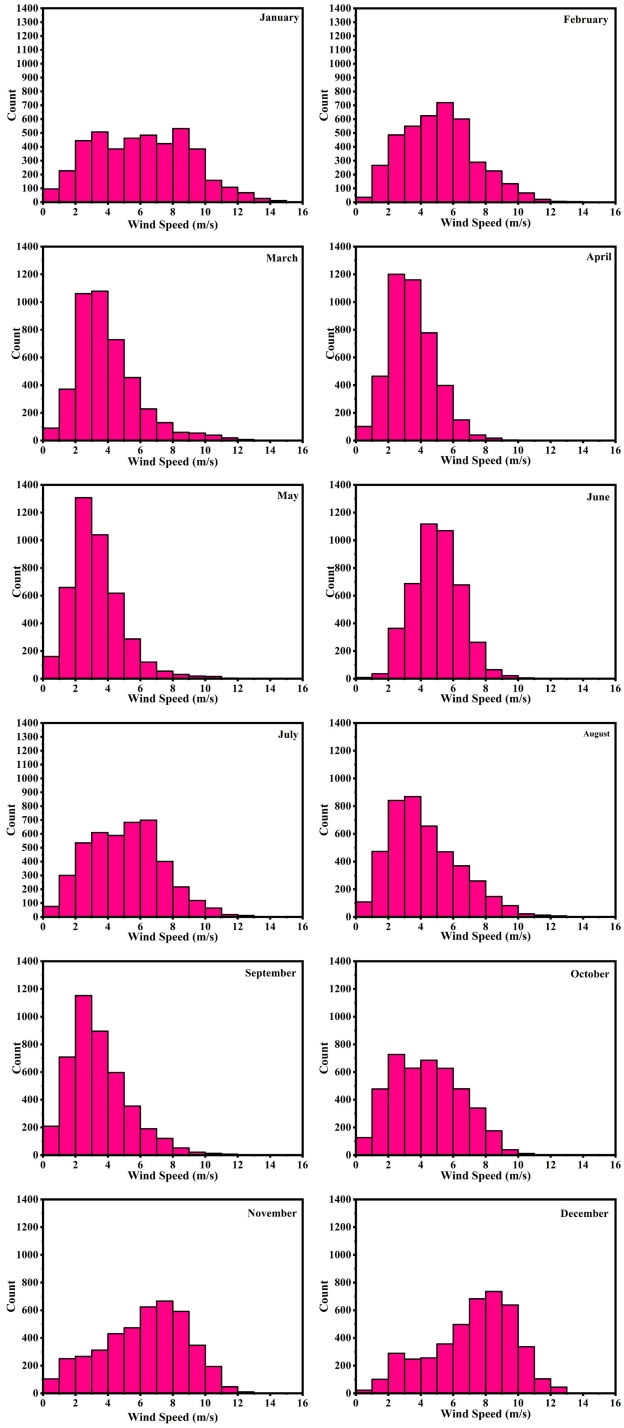

FIGURE 2. Histogram view of annual wind speed for an 8 MW wind farm.

of 6 m/s failed to maintain a higher count. Secondly, a higher frequency count recorded with a low wind speed could not generate higher power, resulting in April, May, September, and October yielding less power following March. This wind speed histogram exhibits a wind pattern based on the frequency count. Overall, December and July recorded higher frequencies of high wind speeds.

Apart from the wind speed, the feeder trip plays an energetic role in deteriorating the wind turbine power fed to the grid. Feeder trips occur because of low and high voltages, and they mainly depend on the nature of the grid voltage. Secondly, annual feeder trips that are higher than 55 times increase the security and warranty issues of the wind turbine. In the selected wind farm, the yearly feeder trip reached 146 times, nearly threefold higher than the manufacturer's guidelines. Figure 3 depicts a detailed view of each month's feeder trip count and duration. It was found that January, February, November, and December recorded lower and higher feeder trips in September and May. The feeder trip during September and May was due to the low wind potential that failed to generate higher power to feed the grid.

On the other hand, the maximum feeder trip duration reached 1800 min in October owing to the low wind speed. In general, integrating BESS with wind farms will not eliminate feeder trips; however, the rate of feeder trips will be reduced. In the general thumb rule, a higher wind speed is attributed to the feeder trip to avoid overvoltage; however, in this case, wind speeds greater than or equal to 14 m/s faced three feeder trips, and 12-14 m/s did not face the feeder trip. Notably, wind speeds of 4-6 m/s and 6-8 m/s faced 58 and 35 times higher feeder trips, respectively. This feeder trip indicated that the voltage in the grid played a significant role in tripping the feeder to protect the grid. In a 24-hour wind farm operational period, higher feeder trips were noted between 06:00 and 09:00, which is 33 times, and following that, 15:00 and 18:00 faced 26 times.

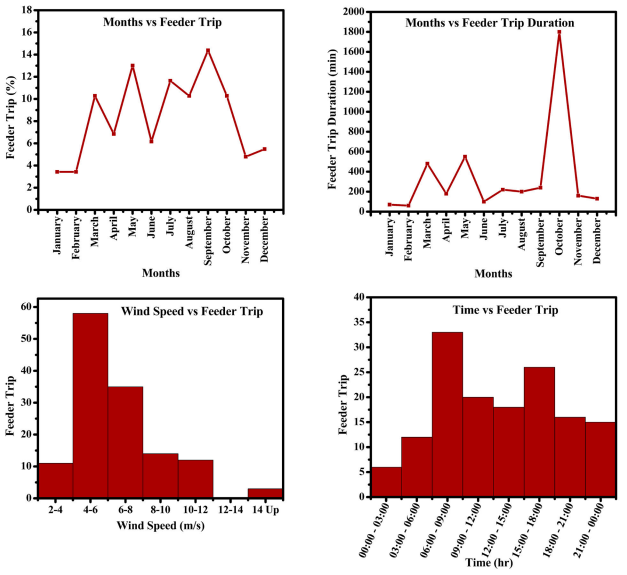

FIGURE 3. Annual feeder trip of an 8 MW wind farm.

The Pearson correlation method was used to understand further the nature of wind speed, the feeder trip count, time duration, energy production, and energy loss. Figure 4 shows that wind speed (WS) strongly correlates negatively with feeder trip count (−0.67576) because higher feeder trips occurred for 4-6 m/s. Secondly, the increase in wind speed has a moderate and weak negative correlation with the feeder trip time duration (FT-T) and energy loss (EL), which are −0.3012 and −0.2287, respectively. An increase in wind speed generates higher power, and it has been found that wind speed has a strong positive correlation (0.7426) with energy production (EP). It is well known that an increase in the feeder trip count (FT-No) increases the energy loss; in this case, the feeder trip count and energy loss have a moderate positive correlation (0.4992). However, the feeder trip duration has a very strong positive correlation with the energy loss, which is 0.9543. The feeder trip count affects the manufacturer warranty claim but is attributed to a moderate correlation with energy loss. An increase in the duration of the feeder trip time increases energy loss and deteriorates the wind farm's performance. The feeder trip duration was worse than the feeder trip count regarding energy loss. To further understand the variability/dispersion of the data used in Figure 4, the standard analytical tool of Standard Deviation (SD) was applied to each variable independently. The deviation of the mean value for wind speed, feeder trip count, and energy loss were 1.2, 5.5, and 9.9, respectively. The annual wind speed and feeder trip counts are dispersed less from the mean value, and the energy loss deviates moderately. However, feeder trip duration and energy production are widely dispersed from the mean values of 283.1 and 695.28, respectively. The reason behind the massive variability in feeder trip duration is that October, March, and May reached maximum durations of 1070, 460, and 410 min, whereas February and January reached maximum durations of 60 and 70 min, respectively. Following this, similar SD patterns were observed for energy production due to high annual energy production fluctuations. Higher SD values were recorded for energy production and feeder trip duration. As mentioned above, the BESS reduces the feeder trip and its duration but cannot feed uninterrupted power to the grid. Following our previous study [32], annual energy generation for different BESS was performed for comparison.

Wind farms without BESS energy generation have a very strong positive correlation with all BESS capacities, as shown in Figure 5. The difference between the annual energy generation with and without the BESS reached a maximum of 2.4 %. A strong positive correlation exists between BESS capacity and the absence of BESS. To further understand the magnitude and dispersion of energy generation, the SD was calculated for wind farms with and without BESS. The wind farm without BESS SD value is 695.28, which is 0.33, 1.41, 3.57, 5.90, and 7.65 SD higher than 1-5 MWh BESS, respectively. An increase in the BESS capacity shows a higher dispersion in energy generation owing to the controller feeder trip duration and count. Second, shifting the wind farm energy generation to meet the load demand favors using more wind farm energy generation. Therefore, it is concluded that 5 MWh BESS with wind farm operations is efficient.

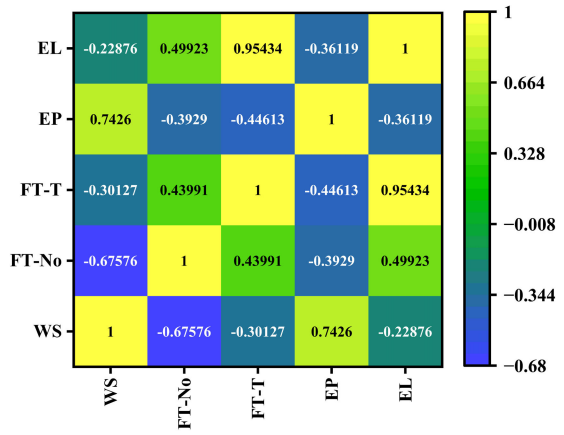

FIGURE 4. Pearson Correlation for 8 MW wind farm energy profile and feeder trip.

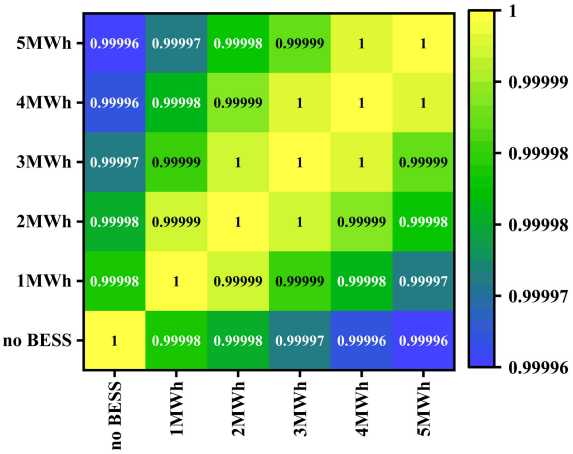

FIGURE 5. Pearson correlation coefficient of 8 MW wind farm using with and without BESS.

This 8 MW wind farm is located within the boundaries of residential villages and industrial areas. This mixed-load consumption zone creates grid voltage issues due to load consumption's unpredictable and discontinuous/intermittent nature. Figure 6 shows the high-load profile correlation plot for grid load consumption and voltage at the wind farm, which is represented as Very Small Power Producer (VSPP), three villages Point of Common Coupling (PCC_01, PCC_02, and PCC_03), and factory (DTA04). The wind farm's nearest connecting load consumption hubs are PCC_02 and PCC_01, which show a very strong positive correlation of 0.989 and 0.998 without BESS (wob). However, DTA04 exhibited a strong negative correlation, which means that the grid voltage at the factory was much lower than the voltage at the wind farm. A significant voltage difference was noted between DTA04 and the villages (PCC_01, PCC_02, and PCC_03).

DTA04 with PCC_01 has a strong negative correlation with a factor of −0.474, which means that the voltage at the factory is lower than that in the village because of high load consumption. Comparatively, other villages also faced a similar trend, with correlations of −0.472 and −0.473. However, the voltage ranges are identical for all the villages, and the correlations are nearly perfectly positive and very strong. That indicates wind farm power generation and grid voltage face complexity in operation without BESS. The load with BESS (wb) depicts correlations of 0.351, −0.983, −1, and −1 for DTA04, PCC_01, PCC_02, and PCC_03, respectively. The grid voltages are within the allowable range for all three villages compared to those without BESS.

On the other hand, PCC_01 (wob) with PCC-01 (wb) has a 0.127 less positive correlation, followed by PCC_02 and PCC_03 with 0.106 and 0.104 correlation differences, respectively. Apart from the villages, wind farms and DTA04 also contained correlation differences of 0.335 and 0.297, respectively. An 8 MW wind farm with a 5 MWh BESS effectively maintained the grid voltage at the wind farm and across the load consumption regions. Table 3 shows the mean and SD for different load consumption regions and wind farms. The SD for BESS clearly defined the deviations; however, it is minor to note that the dataset used in this statistical analysis was in the form of pu to simplify the analysis.

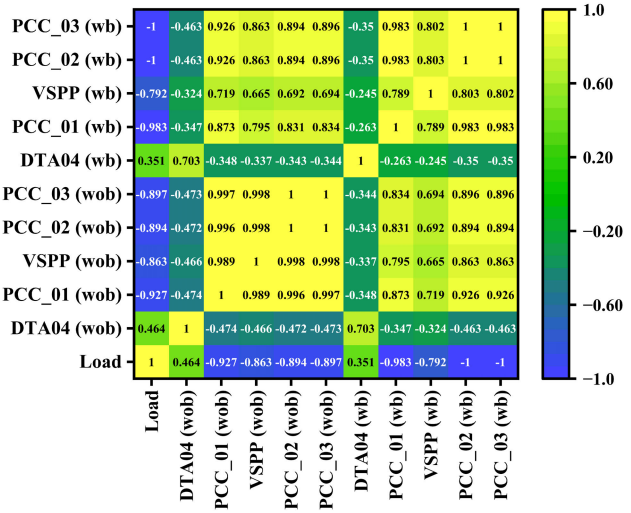

FIGURE 6. Pearson correlation of grid high-load period and different points of grid voltage in the transmission system with and without BESS.

To further understand the benefits of 5 MWh BESS, a low-load demand period was used to analyze the correlation between different regions of the consumer's voltage profile as shown in Figure 7. In this case, the load demand negatively correlated with DTA04 without BESS. On the other hand, PCC_01, PCC_02, and PCC_03 have fewer negative correlations compared to the high load profile. The low voltage at the consumer end causes this massive disruption in correlation. The voltage magnitudes from the wind farm to DTA04, PCC_01, PCC_02, and PCC_03 had positive correlations of 0.322, 0.997, 0.999, and 0.999, respectively. This correlation shows that the voltage magnitudes of the villages and factories follow similar trends to wind farms. The reason behind the same correlation factor of PCC_02

TABLE 3. Statistical analysis of grid high load period and different points of grid voltage in the transmission system using with and without BESS.

Parameter	Mean	SD
Load	2.04571	0.55134
Factory without BESS (DTA04 (wob))	1.03	1.43576E-7
Village 1 without BESS (PCC_01 (wob))	1.04818	0.0049
Wind farm without BESS (VSPP (wob))	1.07586	0.00895
Village 2 without BESS (PCC_02 (wob))	1.07239	0.01007
Village 3 without BESS (PCC_03 (wob))	1.07201	0.01018
Factory with BESS (DTA04 (wb))	1.03	1.02062E-7
Village 1 with BESS (PCC_01 (wb))	1.02291	9.81486E-4
Wind farm with BESS (VSPP (wb))	1.02493	3.78418E-5
Village 2 with BESS (PCC_02 (wb))	1.02154	0.00129
Village 3 with BESS (PCC_03 (wb))	1.02118	0.0014

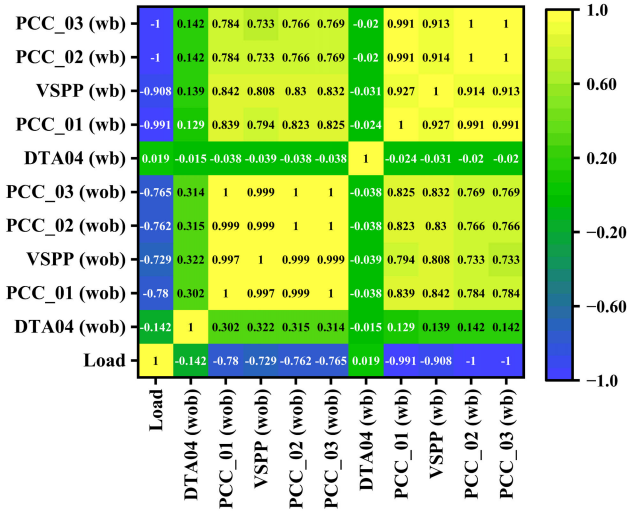

FIGURE 7. Pearson correlation of grid low-load period and different points of grid voltage in the transmission system with and without BESS.

and PCC_03 with the wind farm indicates that the load consumption was less than that of DTA04. In addition, the PCC_01 power transmission line is affected by the DTA04 owing to its high energy consumption. The map of the three villages, wind farm, and DTA04 power transmission network is shown in the Appendix (Figure 8). Second, DTA04 with PCC_01, PCC_02, and PCC_03 showed weak positive correlations within 0.302, 0.315, and 0.314, respectively. DTA04 with other energy consumer villages had a strong negative correlation for the high load profile; however, in this case, the PCC_01, PCC_02, and PCC_03 voltage magnitudes were lower than DTA04, resulting in a weak positive correlation. The integration of 5 MWh BESS for a low-load profile demonstrates that the voltage magnitudes of PCC_01, PCC_02, and PCC_03 are in phase with DTA04.

The wind farm voltage magnitude with three village energy consumers has a very strong positive correlation within the

TABLE 4. Statistical analysis of grid low load period and different points of grid voltage in the transmission system using with and without BESS.

Parameter	Mean	SD
Load	1.66793	0.35095
Factory without BESS (DTA04 (wob))	1.03	1.43576E-7
Village 1 without BESS (PCC_01 (wob))	1.02548	0.00551
Wind farm without BESS (VSPP (wob))	1.02396	0.01036
Village 2 without BESS (PCC_02 (wob))	1.02144	0.01095
Village 3 without BESS (PCC_03 (wob))	1.02116	0.011
Factory with BESS (DTA04 (wb))	1.03	1.02062E-7
Village 1 with BESS (PCC_01 (wb))	1.02596	7.17721E-4
Wind farm with BESS (VSPP (wb))	1.02497	2.6427E-5
Village 2 with BESS (PCC_02 (wb))	1.02244	8.24175E-4
Village 3 with BESS (PCC_03 (wb))	1.02216	8.97478E-4

TABLE 5. Basic parameters of wind farm, BESS, and power purchase details.

Parameters	Value
Wind farm initial investment	824459960 baht/8MW
BESS	75,000,000 baht/5MWh
Annual energy production without BESS	17071670.58 kWh
Annual energy production with BESS	17482742.42 kWh
Discount rate	7.36 %
Wind turbine power purchase	20 years
Feed-in tariff	6.874 baht/kWh (0-10 years) and 3.374 baht/kWh (11-20 years)

ranges of 0.927, 0.914, and 0.913. Notably, the grid voltage in different consumer regions is stabilized with the help of BESS. The SD of the voltage magnitude across the distribution system maintained similar trends, following a high-load profile, as listed in Table 4. Furthermore, it was concluded that 5 MWh BESS efficiently regulates the voltage magnitude for both low- and high-load periods.

IV. ECONOMIC ANALYSIS

An economic analysis was performed for an 8 MW wind farm with and without BESS. Subsequently, a varying cost analysis is performed for only BESS (without a wind farm) to understand the impact on the payback period when the BESS is associated with the wind farm. In Thailand, the power purchase agreement for the wind farm includes two different feed-in tariffs: 6.874 baht/kWh for up to ten years and 3.374 baht/kWh for the remaining ten years, as listed in Table 5. The discount rate is 7.36% as per Thailand's financing regulations. Operation and maintenance (O&M) costs include feeder trip penalties and energy loss, which are applied throughout 20 years of plant operation. Table 6 presents a detailed view of energy generation, O&M, and discounted energy generation. Over 20 years of wind farm

TABLE 6. Basic parameters of wind farm, BESS, and power purchase details.

Year	Discount factor (%)	Feed-in tariff (baht)	Without BESS				With BESS			
			Energy generation (kWh)	Energy generation (baht)	O&M (baht)	Discounted energy generation (kWh)	Energy generation (kWh)	Energy generation (baht)	O&M (baht)	Discounted energy generation (kWh)
1	0.931	6.874	17,071,671	117,345,542	11,520,000	15,901,333	17,482,742	120,171,127	5,760,000	16,284,224
2	0.868	6.874	17,037,527	117,110,851	11,635,200	14,781,604	17,447,777	119,930,784	5,817,600	15,137,533
3	0.808	6.874	17,003,452	116,876,629	11,751,552	13,740,723	17,412,881	119,690,923	5,875,776	14,071,589
4	0.753	6.874	16,969,445	116,642,876	11,869,068	12,773,139	17,378,056	119,451,541	5,934,534	13,080,706
5	0.701	6.874	16,935,506	116,409,590	11,987,758	11,873,689	17,343,300	119,212,638	5,993,879	12,159,598
6	0.653	6.874	16,901,635	116,176,771	12,107,636	11,037,576	17,308,613	118,974,213	6,053,818	11,303,352
7	0.608	6.874	16,867,832	115,944,418	12,228,712	10,260,340	17,273,996	118,736,264	6,114,356	10,507,401
8	0.567	6.874	16,834,096	115,712,529	12,350,999	9,537,835	17,239,448	118,498,792	6,175,500	9,767,498
9	0.528	6.874	16,800,428	115,481,104	12,474,509	8,866,206	17,204,969	118,261,794	6,237,255	9,079,697
10	0.492	6.874	16,766,827	115,250,141	44,799,254	8,241,872	17,170,559	118,025,270	6,299,627	8,440,330
11	0.458	3.374	16,733,294	56,453,113	12,725,247	7,661,502	17,136,218	57,812,458	81,362,623	7,845,984
12	0.426	3.374	16,699,827	56,340,207	12,852,499	7,122,000	17,101,945	57,696,833	6,426,250	7,293,491
13	0.397	3.374	16,666,427	56,227,526	12,981,024	6,620,488	17,067,741	57,581,439	6,490,512	6,779,904
14	0.370	3.374	16,633,095	56,115,071	13,110,835	6,154,291	17,033,606	57,466,276	6,555,417	6,302,481
15	0.345	3.374	16,599,828	56,002,841	13,241,943	5,720,922	16,999,539	57,351,344	6,620,971	5,858,678
16	0.321	3.374	16,566,629	55,890,836	13,374,362	5,318,071	16,965,540	57,236,641	6,687,181	5,446,125
17	0.299	3.374	16,533,496	5,779,054	13,508,106	4,943,586	16,931,609	57,122,168	6,754,053	5,062,624
18	0.279	3.374	16,500,429	55,667,496	13,643,187	4,595,473	16,897,745	57,007,923	6,821,594	4,706,128
19	0.259	3.374	16,467,428	55,556,161	13,779,619	4,271,872	16,863,950	56,893,908	6,889,809	4,374,735
20	0.242	3.374	16,434,493	55,445,048	46,117,415	3,971,058	16,830,222	56,780,120	6,958,708	4,066,678

TABLE 7. Annual revenue, IRR, BCR, PP, and NPV for an 8 MW wind farm.

Parameter	Wind farm without BESS	Wind farm with 5 MWh BESS
Annual revenue (THB)	117,345,542.07	120,171,126.57
IRR	7.74%	7.74%
Payback Period (Year)	7.79	7.89
NPV (THB)	579,908,919	662,613,032
BCR	1.51	1.60

operation, energy generation declined from 17071671 kWh to 16434493 kWh, and for BESS, from 17482742 kWh to 16830222 kWh. The association of BESS was found to enhance 411071 kWh/year by reducing feeder trips. Second, feeder trips significantly impact the O&M cost, resulting in wind farms with 5 MWh BESS being twice as low as those without BESS. This enhancement in O&M and energy generation results in higher discounted energy generation. An increase in energy generation greatly impacts annual revenue, with benefits of 2825584.5 baht/year. Following the annual income, the IRR attained 7.74% for both wind farms with and without BESS, as listed in Table 7. Advantageously, PP with a difference of 0.10 years is noted compared to without BESS. This study indicates that integrating a 5 MWh BESS with an 8 MW wind farm potentially enhanced the power output and economic benefits. The PP of the BESS is strongly dependent on the wind farm feeder trip and reduction in energy loss. Apart from BESS integration by a wind farm, if the Provincial Electricity Authority (PEA) installed the BESS separately to improve the grid voltage, BESS would face severe negative impacts in terms of economic benefits.

IRR and BCRs in negative terms and lower than 1, resulting in PP reaching 26.5 years, which is higher than BESS lifetime

TABLE 8. Sensitivity analysis of a varying BESS investment price for independent installation by PEA.

Financial Parameter	Variation in BESS investment cost							
	100%	90%	80%	70%	60%	50%	40%	30%
NPV (THB)	40,802,665	33,302,665	25,802,665	18,302,665	10,802,665	3,302,665	4,197,334	11,697,334
IRR	-7.88	-6.97	-5.91	-4.64	-3.08	-1.08	1.63	5.68
BCR	0.51	0.56	0.62	0.70	0.80	0.93	1.11	1.38
PP (Year)	26.5	23.9	21.2	18.6	15.9	13.3	10.6	8.0

as listed in Table 8. In this case, the BESS discharged energy calculates the economic benefit. Furthermore, to understand the sensitivity of the PP, variable BESS cost rates are used, such as 90%, 80%, 70%, 60%, 50%, 40%, and 30% from the BESS actual price. It was found that PP for BESS, with a 40% cost rate, nearly reached the life expectancy of BESS, and a 30% cost rate reached 8 years. Overall, it was concluded that 5 MWh BESS with an 8 MW wind farm attained attractive PP and economic benefits compared with the independent installation of BESS (without wind farm authorities).

V. CONCLUSION

In this study, an 8 MW operational wind farm was statistically analyzed using real-time PEA and wind farm data. The main objective of this study is to evaluate the root cause of feeder trips by statistically analyzing the data to avoid O&M costs. Furthermore, a detailed economic analysis was conducted for wind farms with and without BESS. The significant findings of the statistical and economic analyses are as follows.

- The box plot shows that December, July, and June are categorized as having high potential, and March, April, May, September, and October have low potential for wind energy generation.
- A histogram view depicts that 7-9 m/s and 4-5 m/s wind frequencies were noted more than 650 times and 1100 times for December and June, respectively, although a lower frequency count of December delivered a higher energy yield owing to the high wind speed.
- The higher wind speed period of December obtained a low feeder trip; however, October reached 1800 times, which yielded a low energy conversion.
- Wind speed has a weak and moderate negative correlation with feeder trips, and feeder trips are mostly correlated with load consumption and grid voltage. A higher correlation difference was noted for 5 MWh BESS owing to the higher energy yield than that without BESS.
- For high- and low-load demand periods, without BESS, a higher voltage difference was noted between the DTA04 and the wind farm. Integration of the BESS regulated the voltage across all energy consumer ends within the allowable range.
- An 8 MW find farm with BESS attained a PP of 7.89 years, whereas the wind farm alone was 7.79 years. The annual revenue for the wind farm with and without BESS was 117,345,542.07 baht and 120,171,126.57 baht, respectively.
- BESS integration by an individual DTA04/PEA reached 26.5 years of PP, which is 2.65 times higher than the life expectancy of the BESS.
- Furthermore, it is recommended that the BESS be integrated with renewable energy sources to improve energy generation capability and attain an attractive PP.

APPENDIX

See Figure 8.

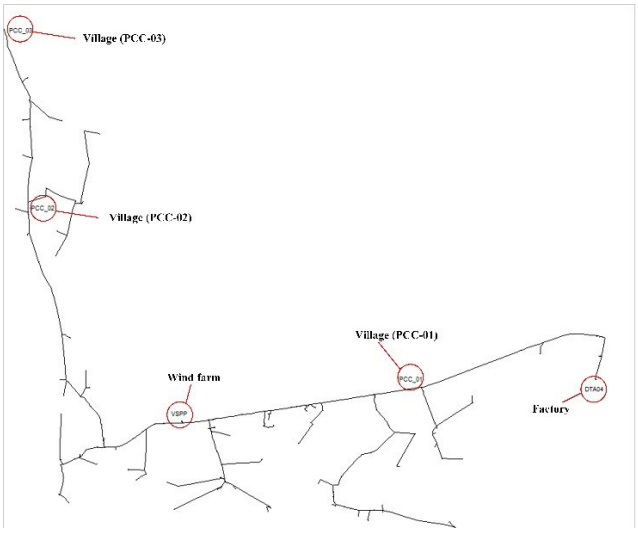

FIGURE 8. Geospatial view of the wind farm, three villages, and factory.

DATA AVAILABILITY

Data and system configuration models are available on request.

ACKNOWLEDGMENT

The authors would like to thank Naresuan University for providing a generous research grant and laboratory facility to conduct this research and also would like to thank the wind farm and PEA for providing the data that is used in this research.

REFERENCES

[1] K. Velmurugan, V. Karthikeyan, S. Kumarasamy, T. Wongwuttanasatian, and C. Sa-Ngiamsak, "Thermal mapping of photovoltaic module cooling via radiation-based phase change material matrix: A case study of a large-scale solar farm in Thailand," *J. Energy Storage*, vol. 55, Nov. 2022, Art. no. 105805.

[2] K. Velmurugan, V. Karthikeyan, K. Sharma, T. B. Korukonda, V. Kannan, D. Balasubramanian, and T. Wongwuttanasatian, "Contactless phase change material based photovoltaic module cooling: A statistical approach by clustering and correlation algorithm," *J. Energy Storage*, vol. 53, Sep. 2022, Art. no. 105139.

[3] Y. F. Nassar, H. J. El-Khozondar, W. El-Osta, S. Mohammed, M. Elnaggar, M. Khaleel, A. Ahmed, and A. Alsharif, "Carbon footprint and energy life cycle assessment of wind energy industry in Libya," *Energy Convers. Manage.*, vol. 300, Jan. 2024, Art. no. 117846.

[4] A. Ali, S. Ali, H. Shaukat, E. Khalid, L. Behram, H. Rani, W. A. Altabey, S. A. Kouritem, and M. Noori, "Advancements in piezoelectric wind energy harvesting: A review," *Results Eng.*, vol. 21, Mar. 2024, Art. no. 101777.

[5] H. Shao, R. Henriques, H. Morais, and E. Tedeschi, "Power quality monitoring in electric grid integrating offshore wind energy: A review," *Renew. Sustain. Energy Rev.*, vol. 191, Mar. 2024, Art. no. 114094.

[6] A. D. A. B. A. Sofian, H. R. Lim, H. S. H. Munawaroh, Z. Ma, K. W. Chew, and P. L. Show, "Machine learning and the renewable energy revolution: Exploring solar and wind energy solutions for a sustainable future including innovations in energy storage," *Sustain. Develop.*, pp. 1–26, Jan. 2024. [Online]. Available: https://onlinelibrary.wiley.com/doi/epdf/10.1002/sd.2885

[7] M. O'Malley, H. Holttinen, N. Cutululis, T. K. Vrana, J. King, V. Gevorgian, X. Wang, F. Rajaei-Najafabadi, and A. Hadjileonidas, "Grand challenges of wind energy science-meeting the needs and services of the power system," *Wind Energy Sci. Discuss.*, vol. 2024, pp. 1–39, Jan. 2024.

[8] A. A. Eladl, S. Fawzy, E. E. Abd-Raboh, A. Elmitwally, G. Agundis-Tinajero, J. M. Guerrero, and M. A. Hassan, "A comprehensive review on wind power spillage: Reasons, minimization techniques, real applications, challenges, and future trends," *Electr. Power Syst. Res.*, vol. 226, Jan. 2024, Art. no. 109915.

[9] J. Giri, N. K. Mishra, A. Patra, and M. K. Shukla, "Control strategies of DFIG technology-based variable-speed wind turbines—A review," *IOP Conf. Ser., Earth Environ. Sci.*, vol. 1285, no. 1, Jan. 2024, Art. no. 012007.

[10] F. H. Malik, M. W. Khan, T. U. Rahman, M. Ehtisham, M. Faheem, Z. M. Haider, and M. Lehtonen, "A comprehensive review on voltage stability in wind-integrated power systems," *Energies*, vol. 17, no. 3, p. 644, Jan. 2024.

[11] H. Li, D. Chen, L. Dong, Z. Li, W. Zhang, and C. Deng, "Summary of research on operation control of electrochemical energy storage power plants for offshore wind power," in *Proc. 9th Int. Conf. Energy Mater. Electr. Eng. (ICEMEE)*, Feb. 2024, pp. 680–689.

[12] J. Close, J. E. Barnard, Y. M. J. Chew, and S. Perera, "A holistic approach to improving safety for battery energy storage systems," *J. Energy Chem.*, vol. 92, pp. 422–439, May 2024.

[13] L. M. S. de Siqueira and W. Peng, "Control strategy to smooth wind power output using battery energy storage system: A review," *J. Energy Storage*, vol. 35, Mar. 2021, Art. no. 102252.

[14] R. Abhinav and N. M. Pindoriya, "Grid integration of wind turbine and battery energy storage system: Review and key challenges," in *Proc. IEEE 6th Int. Conf. Power Syst. (ICPS)*, Mar. 2016, pp. 1–6.

[15] D. K. Panda and S. Das, "Economic operational analytics for energy storage placement at different grid locations and contingency scenarios with stochastic wind profiles," *Renew. Sustain. Energy Rev.*, vol. 137, Mar. 2021, Art. no. 110474.

[16] E. Šunj, M. Šarić, and J. Hivziefendic, "Wind generator transient response analysis and improvement using BESS," *IFAC-PapersOnLine*, vol. 55, no. 4, pp. 322–327, 2022.

[17] M. Jannati, S. H. Hosseinian, B. Vahidi, and G.-J. Li, "ADALINE (ADAptive linear NEuron)-based coordinated control for wind power fluctuations smoothing with reduced BESS (battery energy storage system) capacity," *Energy*, vol. 101, pp. 1–8, Apr. 2016.

[18] M. Jannati and E. Foroutan, "Analysis of power allocation strategies in the smoothing of wind farm power fluctuations considering life-time extension of BESS units," *J. Cleaner Prod.*, vol. 266, Sep. 2020, Art. no. 122045.

[19] P. Liu, W. Zhao, J. Shair, J. Zhang, F. Li, P. Xv, and X. Xie, "Modeling of battery energy storage systems for AGC performance analysis in wind power systems," *Int. J. Electr. Power Energy Syst.*, vol. 155, Jan. 2024, Art. no. 109478.

[20] Y. Song, M. Du, W. Zhao, and H. Lin, "A new integrated regulation strategy and modelling for wind turbine with battery energy storage system," *J. Energy Storage*, vol. 63, Jul. 2023, Art. no. 107111.

[21] R. Villena-Ruiz, A. Honrubia-Escribano, J. Fortmann, and E. Gómez-Lázaro, "Field validation of a standard Type 3 wind turbine model implemented in DIgSILENT-PowerFactory following IEC 61400-27-1 guidelines," *Int. J. Elect. Power Energy Syst.*, vol. 116, Jan. 2020, Art. no. 105553.

[22] N. Manjul and M. S. Rawat, "Transient stability analysis of wind integrated power network using STATCOM and BESS using DIgSILENT PowerFactory," in *Proc. 7th Int. Conf. Adv. Energy Res.* Cham, Switzerland: Springer, 2021, pp. 525–536.

[23] H. Alsharif, M. Jalili, and K. N. Hasan, "A frequency stability analysis for BESS placement considering the loads and wind farms locations," in *Proc. IEEE PES 14th Asia–Pacific Power Energy Eng. Conf. (APPEEC)*, Nov. 2022, pp. 1–5.

[24] I. I. Emon, A. R. Jowel, and A. Jawad, "Participation of battery energy storage system for frequency control in wind dominated power systems: An analytical approach," *Energy Rep.*, vol. 10, pp. 1268–1286, Nov. 2023.

[25] M. Eidiani, "Modeling renewable energy resources using DIgSILENT PowerFactory software," in *Power Systems Operation With 100% Renewable Energy Sources*, S. Chenniappan, S. Padmanaban, and S. Palanisamy, Eds. Amsterdam, The Netherlands: Elsevier, 2024, pp. 165–202.

[26] J. Boyle, T. Littler, and A. M. Foley, "Coordination of synthetic inertia from wind turbines and battery energy storage systems to mitigate the impact of the synthetic inertia speed-recovery period," *Renew. Energy*, vol. 223, Mar. 2024, Art. no. 120037.

[27] S. Galvani, A. Bagheri, M. Farhadi-Kangarlu, and N. Nikdel, "A multi-objective probabilistic approach for smart voltage control in wind-energy integrated networks considering correlated parameters," *Sustain. Cities Soc.*, vol. 78, Mar. 2022, Art. no. 103651.

[28] A. A. Youssef, S. Barakat, E. Tag-Eldin, and M. M. Samy, "Islanded green energy system optimal analysis using PV, wind, biomass, and battery resources with various economic criteria," *Results Eng.*, vol. 19, Sep. 2023, Art. no. 101321.

[29] H. Niaz, M. Zarei, M. H. Shams, W. Won, and J. J. Liu, "Curtailment to cashflow: Exploring BESS and hydrogen for renewable energy profitability," *J. Energy Storage*, vol. 77, Jan. 2024, Art. no. 109990.

[30] N. A. S. Elminshawy, S. Diab, Y. E. S. Yassen, and O. Elbaksawi, "An energy-economic analysis of a hybrid PV/wind/battery energy-driven hydrogen generation system in rural regions of Egypt," *J. Energy Storage*, vol. 80, Mar. 2024, Art. no. 110256.

[31] E. Lobato, L. Sigrist, A. Ortega, A. González, and J. M. Fernández, "Battery energy storage integration in wind farms: Economic viability in the Spanish market," *Sustain. Energy, Grids Netw.*, vol. 32, Dec. 2022, Art. no. 100854.

[32] R. Ngoenmeesri, S. Chidaruksa, R. Wangkeeree, and C. Sirisamphanwong, "Power quality enhancement for Thailand's wind farm using 5 MWh Li-ion battery energy storage system," *Heliyon*, vol. 9, no. 11, Nov. 2023, Art. no. e22029.

[33] N. S. Rayit, J. I. Chowdhury, and N. Balta-Ozkan, "Techno-economic optimisation of battery storage for grid-level energy services using curtailed energy from wind," *J. Energy Storage*, vol. 39, Jul. 2021, Art. no. 102641.

[34] Z. Yao, K. Wu, Y. Zhang, Q. Yan, J. Shi, J. Sun, H. Hu, B. Li, and J. Ye, "Optimal allocation and economic analysis of energy storage capacity of new energy power stations considering the full life cycle of energy storage," in *Proc. IEEE 6th Conf. Energy Internet Energy Syst. Integr. (EI2)*, Nov. 2022, pp. 2592–2599.

[35] K. Wang, S. Zhou, S. Lu, and Z. Li, "Economic analysis of energy storage power station applied to distribution network," in *Proc. 2nd Int. Conf. Electr. Eng. Control Sci. (IC2ECS)*, Dec. 2022, pp. 487–491.

[36] S. Schopfer, V. Tiefenbeck, and T. Staake, "Economic assessment of photovoltaic battery systems based on household load profiles," *Appl. Energy*, vol. 223, pp. 229–248, Aug. 2018.

[37] H. Yin, J. Zhang, C. Wang, and X. Hu, "Economic and technical comparison of energy storage technologies for renewable accommodation," in *Proc. 4th Int. Conf. Electr. Eng. Control Technol. (CEECT)*, Dec. 2022, pp. 1120–1125.

[38] T. R. Ayodele, T. C. Mosetlhe, A. A. Yusuff, M. Ntombela, and K. Moloi, "Economic comparison of PV/wind hybrid energy system with different energy storage technologies," in *Proc. IEEE PES/IAS PowerAfrica*, Aug. 2021, pp. 1–5.
[39] S. B. Wali, M. A. Hannan, P. J. Ker, M. S. A. Rahman, S. K. Tiong, R. A. Begum, and T. M. I. Mahlia, "Techno-economic assessment of a hybrid renewable energy storage system for rural community towards achieving sustainable development goals," *Energy Strategy Rev.*, vol. 50, Nov. 2023, Art. no. 101217.
[40] G. Fambri, P. Marocco, M. Badami, and D. Tsagkrasoulis, "The flexibility of virtual energy storage based on the thermal inertia of buildings in renewable energy communities: A techno-economic analysis and comparison with the electric battery solution," *J. Energy Storage*, vol. 73, Dec. 2023, Art. no. 109083.
[41] Z. Medghalchi and O. Taylan, "A novel hybrid optimization framework for sizing renewable energy systems integrated with energy storage systems with solar photovoltaics, wind, battery and electrolyzer-fuel cell," *Energy Convers. Manage.*, vol. 294, Oct. 2023, Art. no. 117594.
[42] C. Jamroen and P. Vongkoon, "The role of state-of-charge management in optimal techno-economic battery energy storage sizing for off-grid residential photovoltaic systems," *J. Energy Storage*, vol. 72, Nov. 2023, Art. no. 108246.
[43] J. S. Nirbheram, A. Mahesh, and A. Bhimaraju, "Techno-economic optimization of standalone photovoltaic-wind turbine-battery energy storage system hybrid energy system considering the degradation of the components," *Renew. Energy*, vol. 222, Feb. 2024, Art. no. 119918.
[44] D. Emad, M. A. El-Hameed, and A. A. El-Fergany, "Optimal techno-economic design of hybrid PV/wind system comprising battery energy storage: Case study for a remote area," *Energy Convers. Manage.*, vol. 249, Dec. 2021, Art. no. 114847.
[45] G. Zhou, Z. Wang, S. Wang, W. Jiang, and J. Cai, "Capacity optimization configuration of wind-solar IES considering hydrogen energy storage," in *Proc. IEEE 2nd Int. Conf. Mobile Netw. Wireless Commun. (ICMNWC)*, Dec. 2022, pp. 1–6.
[46] H. Liu, X. Ji, J. Kang, and W. Wang, "Coordinated control strategy of wind power fluctuation suppression and frequency modulation based on hybrid energy storage system," in *Proc. IEEE 4th Int. Electr. Energy Conf. (CIEEC)*, May 2021, pp. 1–6.
[47] A. Nkundibiza and P. M. Moses, "Design and optimization of hybrid electrical energy storage system for grid connected wind energy," in *Proc. IEEE PES/IAS PowerAfrica*, Aug. 2022, pp. 1–5.
[48] Y. Wan, X. Liu, X. Wu, and Q. Liu, "Economic analysis method for peak shaving of wind storage combined system considering energy storage participating in peak shaving," in *Proc. Int. Conf. Intell. Transp., Big Data Smart City (ICITBS)*, Jan. 2020, pp. 431–434.
[49] J. Bian, Z. Zhou, Z. Yu, J. Yu, K. Gou, and H. Chen, "Economic dispatch of a virtual power plant with Wind-photovoltaic-storage considering demand response," in *Proc. 8th Int. Conf. Power Renew. Energy (ICPRE)*, Sep. 2023, pp. 955–964.
[50] J. Xiaoliang, L. Zhiming, and Z. Yongjie, "Economic optimal scheduling for integrated energy system with offshore wind power," in *Proc. 4th Int. Conf. Electr. Eng. Control Technol. (CEECT)*, Dec. 2022, pp. 847–851.
[51] M. J. Rahman, T. Tafticht, and M. L. Doumbia, "Frequency control for a high penetration wind-based energy storage system in the power network," in *Proc. IEEE Electr. Power Energy Conf. (EPEC)*, Nov. 2020, pp. 1–6.
[52] A. Haiyun, L. Wenbo, and J. Yuqiao, "Optimal capacity allocation method of multi-types of energy storage for wind power plant," in *Proc. IEEE Int. Conf. Power Sci. Technol. (ICPST)*, May 2023, pp. 838–843.
[53] C. Yuming, J. Peng, M. Gaojun, W. Yao, and L. Tiantian, "Optimal capacity configuration of hybrid energy storage system considering smoothing wind power fluctuations and economy," *IEEE Access*, vol. 10, pp. 101229–101236, 2022.
[54] M. Nasser, T. F. Megahed, S. Ookawara, and H. Hassan, "Performance evaluation of PV panels/wind turbines hybrid system for green hydrogen generation and storage: Energy, exergy, economic, and enviroeconomic," *Energy Convers. Manage.*, vol. 267, Sep. 2022, Art. no. 115870.
[55] J. A. Bennett, J. G. Simpson, C. Qin, R. Fittro, G. M. Koenig, A. F. Clarens, and E. Loth, "Techno-economic analysis of offshore isothermal compressed air energy storage in saline aquifers co-located with wind power," *Appl. Energy*, vol. 303, Dec. 2021, Art. no. 117587.
[56] U. Singh and M. Rizwan, "SCADA system dataset exploration and machine learning based forecast for wind turbines," *Results Eng.*, vol. 16, Dec. 2022, Art. no. 100640.
[57] E. Gonzalez, J. Tautz-Weinert, J. J. Melero, and S. J. Watson, "Statistical evaluation of SCADA data for wind turbine condition monitoring and farm assessment," *J. Phys., Conf. Ser.*, vol. 1037, Jun. 2018, Art. no. 032038.

RATTAPORN NGOENMEESRI received the B.S. degree in civil engineering from the King Mongkut's Institute of Technology North Bangkok, Thailand, in 2001, and the M.S. degree in renewable energy from the School of Renewable Energy Technology, Naresuan University. Phitsanulok, Thailand, in 2011, where he is currently pursuing the Ph.D. degree with the Unit of Business Development and Academic Services in Renewable Energy System Innovation, Faculty of Science. His main research interests include civil technology, solar photovoltaic applications, and wind energy technologies.

SIRINUCH CHINDARUKSA received the B.S. degree in physics from Srinakharintharawirot University, Phitsanulok, Thailand, in 1988, the M.S. degree in energy technology from the King Mongkut's Institute of Technology, Thonburi, Bangkok, Thailand, in 1993, and the Ph.D. degree. She is currently an Assistant Professor with the Department of Physics, Faculty of Science, Naresuan University, Phitsanulok. She has published numerous research articles in national and international journals. Her research interests include solar thermal applications, thermoelectric generators, and energy storage materials.

RABIAN WANGKEEREE received the Ph.D. degree from the Faculty of Science, Naresuan University, Phitsanulok, Thailand, in 2007. He is currently a Full Professor with the Department of Mathematics, Faculty of Science, Naresuan University. He has authored about 121 articles. His research has appeared in the *Journal of Optimization Theory and Applications*, *Journal of Global Optimization*, *Optimization Letters*, *Journal of Mathematical Analysis and Applications*, *Optimization*, and *Applied Mathematics Letters*. His research interests include optimization problems, optimality conditions, artificial intelligence, and machine learning.

CHATCHAI SIRISAMPHANWONG has thrived as an Associate Professor with the Department of Physics, Naresuan University, situated within the esteemed Faculty of Science, since completing the Ph.D. degree. With a prolific publication history spanning national and international journals, he has secured substantial research funding. His expertise lies in groundbreaking research areas, including solar photovoltaics, wind energy, hydrogen energy, and microgrid systems, making significant contributions to sustainable technology. Beyond academia, he actively engages as a technical advisor for multiple industries in Thailand, utilizing his expertise to drive innovation and tackle industry challenges head-on. Through his interdisciplinary approach and unwavering commitment to research excellence, he continues to shape the future of renewable energy technologies, leaving an indelible mark on both academic and industrial fronts.